

Mössbauer isomer shifts in $^{67}\text{Zn}^{++}$ and $^{61}\text{Ni}^{++}$ nuclei*

Keshav N. Shrivastava[†]

Department of Physics, University of California, Santa Barbara, California 93106

(Received 18 August 1975; revised manuscript received 10 November 1975)

Mössbauer charge density for $^{61}\text{Ni}^{++}$ ($3d^8$) is calculated using Hartree-Fock wave functions. All the core s functions ϕ_{ns} ($n = 1, 2,$ and 3) of Ni^{++} and their overlaps with six O^{--} arranged in an octahedron corresponding to NiO are calculated as a function of interatomic distance R . Similar calculations for $^{67}\text{Zn}^{++}$ in a tetrahedral environment of O^{--} ions, appropriate to ZnO , are also performed. It is found that the isomer shift is given approximately by a "power law" $\sim R^{-7}$.

INTRODUCTION

The isomer shift of Mössbauer lines was discovered by Kistner and Sunyar,¹ who noted a velocity shift in the recoil-free emission and resonant absorption of the 14.4-keV nuclear γ ray of ^{57}Fe in Fe_2O_3 compared with that in stainless steel. They also observed that the s electrons are in effect removed in going from ^{57}Fe in metal to ^{57}Fe in Fe_2O_3 , and that a charge radius smaller for $^{57}\text{Fe}^m$ in the excited state than for ^{57}Fe in its ground state would produce a shift in the correct direction. Using a classical form for the nuclear potential for a finite-size nucleus, this shift can be written²

$$\Delta S^i = (4\pi c Z e^2 r_N \delta r_N / 5 E_\gamma) |\psi(0)|^2, \quad (1)$$

where e is the electronic charge, Ze is the nuclear charge, r_N is the nuclear radius, δr_N is the change in nuclear radius upon emission, c is the velocity of light, E_γ is the γ -ray energy, and $\psi(0)$ is the electronic wave function at the site of the nucleus which determines the electronic charge density $e|\psi(0)|^2$. A good knowledge of the charge density is necessary for proper calibration of the spectra and for the determination of the change δr_N in the nuclear radius. The electronic probability density $|\psi(0)|^2$ at the nucleus is, however, not well known and is significantly altered in the solid as compared with the free-ion value. Some of the effects that have been confirmed include the following:

Overlap effect. It was first demonstrated by Flygare and Hafemeister³ that the effect of overlap of the electronic wave functions of the Mössbauer nuclei with those of the nearest-neighbor atoms produced important changes in the charge density. However, their work was limited to $^{129}\text{I}^-$ only. Later, Simaňek and co-workers⁴ extended the calculations of these overlap effects to ^{57}Fe nuclei.

Covalency effect. Since the electrons of the neighboring atoms may be partially transferred onto the vacant orbits of the Mössbauer atom and

vice versa, this covalency effect alters the s amplitudes at the site of the nucleus through the Coulomb interaction.

Potential distortion. Walch and Ellis⁵ have considered some of the possible terms which affect the charge density through the change in local potential for the case of ^{57}Fe .

Relativistic effect. The electronic charge densities obtained from the solution of the Dirac equation are different from those obtained from the nonrelativistic Schrödinger equation. The Dirac-Fock values appear to be consistently larger than the Hartree-Fock values, which are not too easily predicted because of the difficulty in defining the boundary conditions.⁶ Relativistic calculations for the core s functions have been performed for ^{57}Fe by Trautwein *et al.*⁷

Phonon-induced effect. The changes in the electronic charge density as a result of the spin-phonon interaction have been calculated by the present author^{8,9} and realized in the experiments performed by Perkins and Hazony,¹⁰ Brunot,¹¹ and Kalvius *et al.*¹² in ^{57}Fe and ^{151}Eu nuclei.

There are some further effects, such as the expansion of wave functions in going from the free ion to the solid state, which are not investigated.

In the present paper, we calculate the effect of the overlap of the central-ion functions with those of the nearest-neighbor atoms for $^{61}\text{Ni}^{++}$ in the configuration $3d^8$ for the octahedral NiO and for $^{67}\text{Zn}^{++}(3d^{10})$ in the tetrahedral ZnO , which dominates over other effects. Although experimental measurements of the isomer shift of ^{61}Ni in several compounds have been performed^{13,14} and efforts have been made⁶ to obtain the relative change in the nuclear size, overlap calculations have not been done before. In the case of $^{67}\text{Zn}^{++}$, the Mössbauer effect being weak, no shifts have been measured properly, although the effect itself has been detected by several workers¹⁵⁻²² and experiments on the line shift are feasible. We present the first calculation of the Mössbauer charge densities for

$^{67}\text{Zn}^{++}$ nuclei, including the effect of nearest-neighboring O^{2-} atoms as in ZnO , using an overlap model. From our calculations an interesting "law" of the dependence of the isomer shift on the interatomic separation emerges, namely, $\Delta S^i \sim R^{-7}$.

$^{61}\text{Ni}^{++}$ IN NiO

We present a Hartree-Fock calculation of charge density for $^{61}\text{Ni}^{++}$ in an octahedron of O^{2-} ions, as in NiO , including the overlap of Ni^{2+} s functions with six nearest-neighboring atoms.

For $^{61}\text{Ni}^{2+}$ the Mössbauer energy is 67.4 keV and the relative change in the nuclear size is of the order of $\delta r_N/r_N \approx 10^{-4}$. The isomer shift is determined by the amplitudes of the electronic wave function at the site of the nucleus. Only the s functions have nonzero amplitudes at the nucleus; thus they are the only ones that need be considered. However, there are significant overlaps of these functions with those of the nearest-neighboring atoms in the solid. We consider a $\text{Ni}^{2+}(3d^8)$ ion surrounded by six O^{2-} ions arranged on the centers of six surface planes of a cube with a Ni^{2+} ion at the cube center. The local symmetry is then octahedral and all functions are required to transform as the irreducible representations of the octahedral group. The $3d$ functions transform as t_{2g} and e_g . The wave functions of the six O^{2-} ions have to be linearly combined to transform as the irreducible representations of the octahedral group. The $e_g(3d)$ mix with s and p_σ ($p_z = Y_1^0$, $l=1$, $m=0$) functions of the nearest neighbor, while the $t_{2g}(3d)$ mix with the p_π combination of $p_x = 1/\sqrt{2}(-Y_1^1 + Y_1^{-1})$ and $p_y = i/\sqrt{2}(Y_1^1 + Y_1^{-1})$. The bonding orbitals which are dominantly on the nearest-neighboring atoms are orthogonal to the antibonding orbitals transforming like e_g and t_{2g} . All of these functions have almost vanishing amplitudes at the site of the central nucleus of Ni^{2+} . The only functions which give large contributions to the Mössbauer charge densities are ϕ_{1s} , ϕ_{2s} , and ϕ_{3s} of Ni^{2+} . They overlap with linear combi-

nations of O^{2-} functions s and p_σ , transforming as the A_{1g} representation of the octahedral group. Ignoring the charge transfer within the framework of an overlap model,⁸

$$|\Psi(0)|^2 \approx \sum_n |\phi_{ns}(0)|^2 \left(1 + \sum_k S_{nsk}^2\right), \quad (2)$$

where the sum over n is over all s functions of the Ni^{2+} ion which are doubly occupied. The sum over k is over all neighbors, which are six O^{2-} in our problem. The overlap integrals

$$S_{nsk} = \langle \phi_{ns} | \chi_k(\text{O}^{2-}) \rangle \quad (3)$$

give the mixing of the core s functions with those of nearest neighbors of appropriate symmetry. We use the Ni^{2+} Hartree-Fock wave functions from the work of Clementi and Roetti²³ and the O^{2-} functions from Watson's paper.²⁴ All of the pertinent overlap integrals which we computed using a computer program written by Switendick and Carbatto²⁵ are given in Table I and the core s electron probability densities are given in Table II. As the integrals are sensitive functions of interatomic separation, this parameter is varied from 1.8 to 4.0 Å. Except for the separation, which is given in Å all other values are in atomic units. The integration is reliable up to six places after the decimal point, although eight digits are shown by the computer output. For an interatomic separation of 1.8 Å,

$$\begin{aligned} 12|\phi_{1s}(0)|^2 \langle \phi_{1s} | \chi_{2s} \rangle^2 &= 0.06, \\ 12|\phi_{2s}(0)|^2 \langle \phi_{2s} | \chi_{2s} \rangle^2 &= 0.28, \\ 12|\phi_{3s}(0)|^2 \langle \phi_{3s} | \chi_{2s} \rangle^2 &= 1.57, \\ 12|\phi_{1s}(0)|^2 \langle \phi_{1s} | \chi_{2p} \rangle^2 &= 1.10, \\ 12|\phi_{2s}(0)|^2 \langle \phi_{2s} | \chi_{2p} \rangle^2 &= 5.21, \\ 12|\phi_{3s}(0)|^2 \langle \phi_{3s} | \chi_{3s} \rangle^2 &= 17.42, \end{aligned} \quad (4)$$

where a factor of 6 arises from six neighbors and a factor of 2 arises from the double occupancy of the core s functions. The total 25.64 a.u. of the

TABLE I. Overlap integrals between core s functions of Ni^{2+} ϕ_{ns} and the $2s$ and $2p$ functions $\chi_{n,s,p}$ of O^{2-} as a function of interatomic separation.

R (Å)	$\langle \phi_{1s} \chi_{2p} \rangle$	$\langle \phi_{1s} \chi_{2s} \rangle$	$\langle \phi_{2s} \chi_{2p} \rangle$	$\langle \phi_{2s} \chi_{2s} \rangle$	$\langle \phi_{3s} \chi_{2p} \rangle$	$\langle \phi_{3s} \chi_{2s} \rangle$
1.8	-0.003 686 09	-0.000 831 11	0.026 211 33	0.006 077 75	0.128 195 17	0.038 523 78
2.0	-0.002 641 81	-0.000 470 91	0.018 817 95	0.003 446 96	0.094 209 97	0.022 680 37
2.2	-0.001 906 38	-0.000 266 35	0.013 594 47	0.001 951 12	0.069 221 91	0.013 237 31
2.5	-0.001 185 46	-0.000 112 50	0.008 459 83	0.000 824 83	0.043 753 58	0.005 809 92
3.0	-0.000 563 53	-0.000 026 40	0.004 020 45	0.000 193 78	0.020 949 36	0.001 431 08
3.5	-0.000 284 02	-0.000 006 13	0.002 024 74	0.000 045 00	0.010 511 70	0.000 343 82
4.0	-0.000 149 61	-0.000 001 42	0.001 065 92	0.000 010 40	0.005 504 91	0.000 081 32

TABLE II. Core s electron Hartree-Fock charge densities for $\text{Ni}^{2+}(3d^8)$.

	1s	2s	3s
$\phi_{ns}(0)$	-82.14	-25.148	9.40
$ \phi_{ns}(0) ^2$	6746.94	632.42	88.36

above is not negligible compared with $|\phi_{3s}(0)|^2 = 88.36$ a.u. We therefore conclude that the isomer shift produced by the overlap effect is not small. The dominant terms are given in Table III.

The isomer shift then consists of two types of terms,

$$\Delta S^i = K \left(\sum_n |\phi_{ns}(0)|^2 + \sum_i a_i \right), \quad (5)$$

where

$$K = 4\pi c Z e^2 r_N \delta r_N / 5E_\gamma. \quad (6)$$

The first term $\sum_n |\phi_{ns}(0)|^2 = 14935.44 a_0^{-3}$, after introducing a factor of 2 to take into account the spin double occupancy, is a constant. If we now multiply it by a relativistic correction factor of 1.34, we obtain $1367.38 \times 10^{26} \text{ cm}^{-3}$. This value is much larger than the free-ion value $1329.63 \times 10^{26} \text{ cm}^{-3}$ calculated by Love *et al.*⁶ from the Herman-Skillman wave functions. These workers⁶ also indicate the difficulties in defining the boundary conditions for performing the integration. Using the Wigner-Seitz model, the s amplitude is found to vary with the Wigner-Seitz radius r_{WS} . For r_{WS} of 0.529, 1.587, and 10.583 Å, the electronic amplitudes for the $3d^8$ configuration are calculated to be 1325.92, 1329.68, and $1329.58 \times 10^{26} \text{ cm}^{-3}$, respectively. These values are smaller than our calculated value of $1367.38 \times 10^{26} \text{ cm}^{-3}$. It may be noted that this value, calculated from Watson's wave functions,²⁶ is about $1364.65 \times 10^{26} \text{ cm}^{-3}$.

The second term in (5),

$$\sum_i a_i = \sum_n \sum_k |\phi_{ns}(0)|^2 S_{nsk}^2 \quad (7)$$

is a function of interatomic separation R . The overlap contribution $\sum_i a_i$ is plotted in Fig. 1. It is found that

$$\frac{-\partial \ln(\Delta S^i)}{\partial \ln R} \approx 7.0 \quad (8)$$

at $R \approx 2 \text{ Å}$, so that the isomer shift appears to vary approximately as R^{-7} in our model, although the predicted variation is, in fact, more complicated than just a "power law." At large distances

TABLE III. Dominant overlap contributions to charge densities as a function of interatomic separation R in NiO. $a_1 = 12|\phi_{1s}(0)|^2 \langle \phi_{1s} | \chi_{2p} \rangle^2$, $a_2 = 12|\phi_{2s}(0)|^2 \langle \phi_{2s} | \chi_{2p} \rangle^2$, $a_3 = 12|\phi_{3s}(0)|^2 \langle \phi_{3s} | \chi_{2p} \rangle^2$, $a_4 = 12|\phi_{3s}(0)|^2 \langle \phi_{3s} | \chi_{2s} \rangle^2$.

R (Å)	a_1	a_2	a_3	a_4	$\sum_i a_i$
1.8	1.1	5.21	17.43	1.57	25.31
2.0	0.57	2.69	9.41	0.55	13.22
2.2	0.29	1.40	5.08	0.19	6.96
2.5	0.11	0.54	2.03	0.04	2.72
3.0	0.03	0.12	0.47	0.002	0.62
3.5	0.01	0.03	0.12	0.0001	0.16

the power is closer to 9 than to 7, so that the approximate power is $\sim 8.0 \pm 1.0$.

$^{67}\text{Zn}^{++}$ IN ZnO

There has been a considerable amount of interest in the study of the ^{67}Zn 93.3-keV transition¹⁵⁻²². The isomer shift which is inversely proportional to the γ -ray energy and directly proportional to the nuclear charge Ze is smaller for the 93.3-keV γ ray of ^{67}Zn than for the 67.4-keV γ ray of ^{61}Ni by a factor of about 0.79. The Zn^{++} ion, being in the electronic configuration $3d^{10}$, forms a singlet ground state with $S=0$, $L=0$, and $J=0$.

We write the core s functions ϕ_{ns} of Zn^{++} , including that combination of $\chi_i(\text{O}^{2-})$ wave functions that transforms as the A_{1g} irreducible representation of the tetrahedral group, as

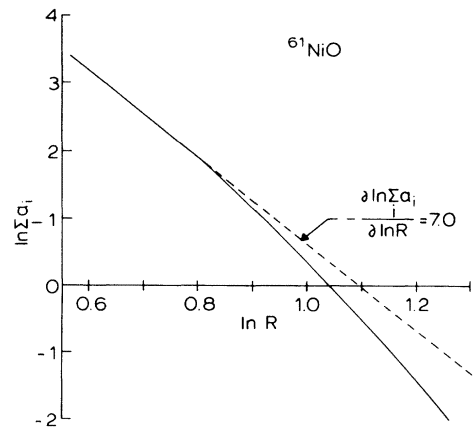


FIG. 1. Natural double-logarithmic plot of predicted overlap contribution to the Mössbauer isomer shift in ^{61}NiO as a function of interatomic separation. At small separations an inverse seventh power is indicated by the dashed line. At large distances the power is about inverse ninth, so that the behavior of isomer shift is obtained by a power law of $R^{-8 \pm 1}$.

TABLE IV. Overlap integrals between the core s functions ϕ_{ns} of Zn^{2+} and the O^{2-} $2s$ and $2p$ functions χ_i , in a.u. reliable up to six decimal places.

R (Å)	$\langle \phi_{1s} \chi_{2s} \rangle$	$\langle \phi_{1s} \chi_{2p} \rangle$	$\langle \phi_{2s} \chi_{2s} \rangle$	$\langle \phi_{2s} \chi_{2p} \rangle$	$\langle \phi_{3s} \chi_{2s} \rangle$	$\langle \phi_{3s} \chi_{2p} \rangle$
1.8	-0.000 749 79	-0.003 318 46	-0.005 449 34	-0.023 447 86	0.032 826 33	0.113 686 20
1.9	-0.000 565 07	-0.002 808 64	-0.004 111 17	-0.019 865 92	0.025 132 25	0.097 280 74
2.0	-0.000 424 68	-0.002 377 37	-0.003 092 73	-0.016 830 14	0.019 158 86	0.083 127 14
2.1	-0.000 320 09	-0.002 019 70	-0.002 333 14	-0.014 308 15	0.014 625 80	0.071 182 31
2.2	-0.000 240 61	-0.001 716 92	-0.001 755 20	-0.012 170 11	0.011 123 52	0.060 913 89
2.3	-0.000 180 71	-0.001 462 35	-0.001 319 27	-0.010 370 18	0.008 445 15	0.052 163 47
2.5	-0.000 101 70	-0.001 067 84	-0.000 743 50	-0.007 576 48	0.004 845 48	0.038 378 76
3.0	-0.000 023 89	-0.000 507 68	-0.000 175 14	-0.003 602 10	0.001 182 41	0.018 339 23
3.5	-0.000 005 65	-0.000 255 88	-0.000 040 76	-0.001 814 26	0.000 282 17	0.009 204 47
4.0	-0.000 001 28	-0.000 134 78	-0.000 009 43	-0.000 955 08	0.000 066 42	0.004 824 25

$$\begin{aligned}
\phi_{3s} &= N_{3s} \left(\phi'_{3s} - \sum_i \langle \phi_{3s} | \chi_i \rangle \chi_i \right), \\
\phi_{2s} &= N_{2s} \left(\phi'_{2s} - \sum_i \langle \phi_{2s} | \chi_i \rangle \chi_i \right), \\
\phi_{1s} &= N_{1s} \left(\phi'_{1s} - \sum_i \langle \phi_{1s} | \chi_i \rangle \chi_i \right),
\end{aligned} \tag{9}$$

$$\begin{aligned}
a_1 &= 8 |\phi_{1s}(0)|^2 \langle \phi_{1s} | \chi_{2p} \rangle^2, & a_2 &= 8 |\phi_{2s}(0)|^2 \langle \phi_{2s} | \chi_{2p} \rangle^2, \\
a_3 &= 8 |\phi_{3s}(0)|^2 \langle \phi_{3s} | \chi_{2p} \rangle^2, & a_4 &= 8 |\phi_{3s}(0)|^2 \langle \phi_{3s} | \chi_{2s} \rangle^2, \\
a_5 &= 8 |\phi_{2s}(0)|^2 \langle \phi_{2s} | \chi_{2s} \rangle^2, & a_6 &= 8 |\phi_{1s}(0)|^2 \langle \phi_{1s} | \chi_{2s} \rangle^2,
\end{aligned} \tag{12}$$

where the normalization constants are

$$\begin{aligned}
N_{3s} &= \left(1 + \sum_i |\langle \phi'_{3s} | \chi_i \rangle|^2 \right)^{-1/2}, \\
N_{2s} &= \left(1 + \sum_i |\langle \phi'_{2s} | \chi_i \rangle|^2 \right)^{-1/2}, \\
N_{1s} &= \left(1 + \sum_i |\langle \phi'_{1s} | \chi_i \rangle|^2 \right)^{-1/2}.
\end{aligned} \tag{10}$$

As a result of overlap with nearest neighbors, the orthogonality amongst the ϕ_{ns} is slightly destroyed and is to be reestablished. If we keep only the largest terms, the contribution of overlap effects to the isomer shift is determined by

$$\sum_n |\phi_{ns}(0)|^2 + \sum_i a_i, \tag{11}$$

where the dominant terms are

TABLE V. Core s electron Hartree-Fock charge densities for $\text{Zn}^{++}(3d^{10})$, in a.u.

	1s	2s	3s
$\phi_{ns}(0)$	-91.20	28.14	10.60
$ \phi_{ns}(0) ^2$	8316.83	791.77	112.47

where a factor of 8 arises because of the tetrahedral symmetry in which one considers four neighbors, compared with a factor of 12 arising in octahedral symmetry from six neighbors as in the expression (4). We use the Hartree-Fock wave functions of Zn^{++} from the tables of Clementi and Roetti²³ and those of O^{2-} from Watson's work.²⁴ The calculated values are given in Tables IV–VI. The overlap integrals depend strongly on the interatomic separation. Accordingly, this contribution is calculated by treating the distance between the Zn^{++} and O^{2-} as a variable, as shown in Fig. 2. It is found that for $R \approx 2$ Å, the isomer

TABLE VI. Dominant overlap contributions to charge densities for tetrahedral ZnO as a function of the interatomic separation R .

R (Å)	a_1	a_2	a_3	a_4	a_5	a_6	$\sum_i a_i$
1.8	0.73	3.48	11.63	0.97	0.19	0.04	17.04
1.9	0.53	2.50	8.51	0.57	0.11	0.02	12.23
2.0	0.37	1.79	6.22	0.33	0.06	0.01	8.79
2.1	0.27	1.30	4.56	0.19	0.03	0.01	6.37
2.2	0.19	0.94	3.34	0.11	0.02	0.00	4.61
2.3	0.14	0.68	2.45	0.07	0.01	0.00	3.35
2.5	0.07	0.37	1.33	0.02	0.01	0.00	1.79
3.0	0.02	0.08	0.30	0.00	0.00	0.00	0.40

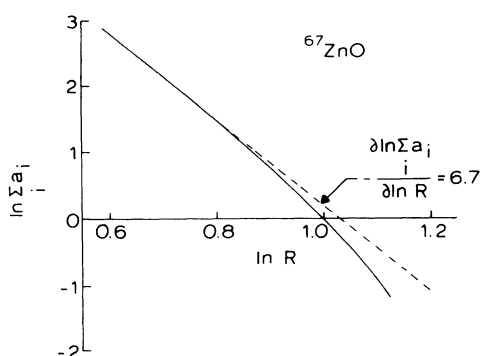


FIG. 2. Predicted behavior of isomer shift of ^{67}Zn as a function of interatomic separation. At small distances the dashed line indicates a slope of 6.7, whereas at larger distances this value changes to about 8.3.

shift arising from the overlap varies as $R^{-6.7}$. This result may be verified by studying the effect of hydrostatic pressure on the Mössbauer spectra or by studying the line positions in several oxide lattices. The result $\Delta S^i \sim R^{-7}$ is also pertinent for predictions of the effect of thermal expansion. The core s contribution 18 442.14 a.u. is constant and predicts a center shift required for proper calibration of velocity.

CONCLUSIONS

We have calculated the Mössbauer charge density for $^{61}\text{Ni}^{2+}$ in NiO and found that as a result of variation of overlap integrals between the core s functions and the nearest-neighbor ligand functions, the isomer shift varies with interatomic separation. For small variations the shift is proportional to the inverse seventh power of interatomic distance. This result predicts an effect of thermal expansion of the host lattice as well as variation of line shift for the same nuclei in going from one material to another.

We have also calculated the Mössbauer charge density for ^{67}Zn in ZnO from first principles. We find that the isomer shift appears to depend on the interatomic separation, and a new power law, R^{-7} , is predicted. This is the first calculation for the Mössbauer charge density in ^{67}Zn , although there are no measurements of this effect to date.

ACKNOWLEDGMENT

I am grateful to Professor Vincent Jaccarino for useful discussions on the power laws in magnetic resonance which resulted in the present work.

*Supported in part by the NSF.

†Present address: Fysisch Laboratorium, Rijksuniversiteit, Sorbonnelaan 4, Utrecht, The Netherlands.

¹O. C. Kistner and A. W. Sunyar, *Phys. Rev. Lett.* **4**, 412 (1960).

²G. K. Wertheim, *The Mössbauer Effect* (Academic, New York, 1964).

³W. H. Flygare and D. W. Hafemeister, *J. Chem. Phys.* **43**, 789 (1965).

⁴E. Simanek and Z. Sroubek, *Phys. Rev.* **163**, 275 (1967); E. Simanek and A. Y. C. Wong, *ibid.* **166**, 348 (1968).

⁵P. F. Walch and D. E. Ellis, *Phys. Rev. B* **7**, 903 (1973).

⁶J. C. Love, F. E. Obenshain, and G. Czjzek, *Phys. Rev. B* **3**, 2827 (1971).

⁷A. Trautwein, F. E. Harris, A. J. Freeman, and J. P. Desclaux, *Phys. Rev. B* **11**, 4101 (1975).

⁸K. N. Shrivastava, *Phys. Rev. B* **1**, 955 (1970).

⁹K. N. Shrivastava, *Phys. Rev. B* **7**, 921 (1973).

¹⁰H. K. Perkins and Y. Hazony, *Phys. Rev. B* **5**, 7 (1972).

¹¹B. Brunot, *J. Chem. Phys.* **61**, 2360 (1974).

¹²G. M. Kalvius, U. F. Klein, and G. Wortmann, *J. Phys. (Paris)* **35**, C6-139 (1974).

¹³U. Erich, *Z. Phys.* **227**, 25 (1969).

¹⁴J. C. Travis and J. J. Spykerman, in *Mössbauer Effect Methodology*, edited by I. Gruverman (Plenum, New York, 1968), Vol. 4, p. 237.

¹⁵P. P. Craig, D. E. Nagle, and D. R. F. Cochran, *Phys. Rev. Lett.* **4**, 561 (1960).

¹⁶D. E. Nagle, P. P. Craig, and D. E. Keller, *Nature* **186**, 707 (1960).

¹⁷V. P. Alfimenkov, Yu. M. Ostanevich, T. Ruskov, A. V. Strelkov, F. L. Shapiro, and W. K. Yen, *Zh. Eksp. Teor. Fiz.* **42**, 1029 (1962) [*Sov. Phys.-JETP* **15**, 713 (1962)].

¹⁸J. Lindgren, *Ark. Fys.* **29**, 553 (1965).

¹⁹H. de Waard and G. J. Perlow, *Phys. Rev. Lett.* **24**, 566 (1970).

²⁰A. I. Beskrovmmii and Yu. M. Ostamevich, *Prib. Tekh. Eksp.* **5**, 54 (1971) [*Instrum. Exp. Tech.* **5**, 1320 (1971)].

²¹G. J. Perlow, L. E. Campbell, L. E. Conroy, and W. Potzel, *Phys. Rev. B* **7**, 4044 (1973).

²²G. J. Perlow, W. Potzel, R. M. Kash, and H. de Waard, *J. Phys. (Paris)* **35**, C6-197 (1974).

²³E. Clementi and C. Roetti, *At. Data Nucl. Data Tables* **14**, 177 (1974).

²⁴R. E. Watson, *Phys. Rev.* **111**, 1108 (1958).

²⁵A. C. Switendick and J. J. Carbatto, MIT Solid State and Molecular Theory Group, Quarterly Progress Report No. 34 (1959) (unpublished); modification by E. Moore and G. Wiederhold (unpublished).

²⁶R. E. Watson, MIT Solid State and Molecular Theory Group, Quarterly Progress Report No. 12 (1958) (unpublished).